

Solution Simplex Clustering for Heterogeneous Federated Learning

Dennis Grinwald^{1,2} Philipp Wiesner³ Shinichi Nakajima^{1,2,4}

Abstract

We tackle a major challenge in federated learning (FL)—achieving good performance under highly heterogeneous client distributions. The difficulty partially arises from two seemingly contradictory goals: learning a common model by aggregating the information from clients, and learning local personalized models that should be adapted to each local distribution. In this work, we propose Solution Simplex Clustered Federated Learning (SosicFL) for dissolving such contradiction. Based on the recent ideas of learning solution simplices, SosicFL assigns a subregion in a simplex to each client, and performs FL to learn a common solution simplex. This allows the client models to possess their characteristics within the degrees of freedom in the solution simplex, and at the same time achieves the goal of learning a global common model. Our experiments show that SosicFL improves the performance and accelerates the training process for global and personalized FL with minimal computational overhead.

1. Introduction

Federated Learning (FL) (McMahan et al., 2017) is a decentralized machine learning paradigm that facilitates collaborative model training across distributed devices while preserving data privacy. However, in typical real applications, non-identically and independently distributed (non-IID) data distributions at clients make it difficult to train well-performing models. To tackle this difficulty, various methods have been proposed, e.g., personalized FL (Kulkarni et al., 2020), clustered FL (Sattler et al., 2020), advanced client selection strategies (Lai et al., 2021), robust aggregation (Pillutla

¹Machine Learning Group, Technische Universität Berlin, 10587 Berlin, Germany ²Berlin Institute for the Foundations of Learning and Data (BIFOLD), 10587 Berlin, Germany ³Distributed and Operating Systems Group, Technische Universität Berlin, 10587 Berlin, Germany ⁴RIKEN Center for AIP, Japan. Correspondence to: Dennis Grinwald <dennis.grinwald@tu-berlin.edu>, Philipp Wiesner <wiesner@tu-berlin.de>, Shinichi Nakajima <nakajima@tu-berlin.de>.

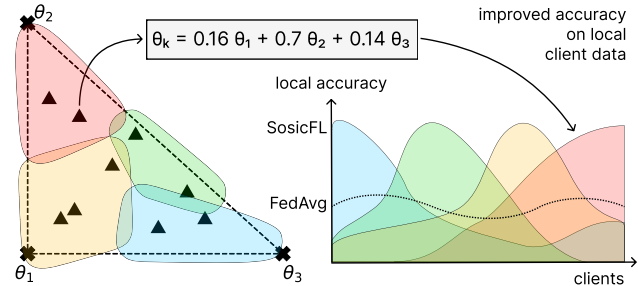


Figure 1. SosicFL clusters clients (\blacktriangle) based on their label distributions, and assigns a subregion (color shadows) of the trained solution simplex to each cluster. During communication rounds, each client uses the solutions within the assigned subregion and sends the gradient information to the server for updating the global solution simplex.

et al., 2022), and federated meta- and multi-task learning approaches (Smith et al., 2017). These methods aim either at training a global model that performs well on the global distribution (Zhao et al., 2018), or, as it is common in personalized FL, at training multiple client-dependent models each of which performs well on its local distribution (Tan et al., 2022). These two aims often pose a trade-off—a model that shows better global performance tends to show worse local performance, and vice versa. In this work, we aim to develop a FL method that improves both global and local performance.

Our approach is motivated by recent research on *mode connectivity* (Draxler et al., 2018; Garipov et al., 2018; Nagarajan & Kolter, 2019)—the existence of low-loss paths in the weight parameter space between independently trained neural networks—and its application to multi-task and continual learning (Mirzadeh et al., 2020). These works show that minima for the same task are typically connected by simple low-loss curves, and that such connectivity benefits training for multi-task and continual learning. More specifically, the authors show that embracing such mode connectivity between models improves accuracy on each task and reduces catastrophic forgetting.

In this paper, we leverage such effects, and propose *Solution Simplex Clustered Federated Learning* (SosicFL), where the solution simplex is shared over the clients in a heterogeneous way. Specifically, SosicFL first clusters the clients

based on their local distributions, and assigns a subregion in the solution simplex to each client. Then, in the training communication rounds, each client participates FL by using the models corresponding to the assigned subregion, and sends back the gradient information for updating the vertices of the global solution simplex. This way, the collaborative training happens through learning the common solution simplex, while the degrees of freedom within the simplex allow the clients to be personalized to their local distributions. Our experiments show that SosisFL outperforms the state-of-the-art methods for global (FedProx in Li et al. (2020)), and personalized (Ditto in Li et al. (2021)) FL approaches without introducing significant computational overhead. Furthermore, we analyze the detailed behavior of SosisFL and observe that it allows personalization within the simplex as designed, which results in low variances of the gradient updates over the clients—evidence that the conflicting updates over the heterogeneous clients are remedied.

Our main contributions are summarized as follows:

- We propose SosisFL, a novel method that shares the solution simplex for absorbing the heterogeneity of the clients, and show its state-of-the-art performance for global and local personalized FL.
- We propose a procedure to represent clients within the solution simplex, and cluster them. Specifically, we used latent Dirichlet allocation (Blei et al., 2003) and Hilbert simplex clustering (Nielsen & Sun, 2019), which exactly match the requirement for subregion assignments.
- We provide detailed empirical analyses of the behavior of SosisFL, which give insights into the mechanisms of our method—why it improves performance compared to the baselines.

Our code is submitted as a supplement and will be made public upon acceptance.

2. Background and Related Work

Here we briefly explain the framework of federate learning and recent research on the mode-connectivity, which are the backbone of our approach. The symbols that we use throughout the paper are listed in Table 1.

2.1. Federated Learning

Assume a federated system where the server has a global model g_0 and the K clients have their local models $\{g_k\}_{k=1}^K$. Federated Learning (FL) aims to obtain the best performing

Table 1. Nomenclature.

Symbol	Description
$l = 1, \dots, L$	Output labels
$t = 1, \dots, T$	Communication rounds
$t' = 1, \dots, T'$	Local training iterations
$k = 1, \dots, K$	Clients
\mathcal{S}^t	The set of clients that participate in round t
$p(k)$	Client data proportion
B	Mini-batch size
γ	Client gradient descent step size
\mathcal{D}_k	Training data of client k
N	Total number of samples
N_k	Number of samples at client k
$P_k(y)$	Label distribution of client k
$p_k(\mathbf{x}, y)$	(joint) data distribution of client k
$\mathbf{w}_0^t \in \mathbb{R}^D$	Global model (parameters) at round t
$\mathbf{w}_k^t \in \mathbb{R}^D$	Client model (weights) at round t
Δ^M	M -dimensional standard simplex
$\theta_1^t, \dots, \theta_{M+1}^t$	solution simplex endpoints at round t
$\alpha \in \Delta^M$	endpoint weights
$\mathbf{w}_\alpha = \sum_{m=1}^M \alpha_m \theta_m$	Model parameters at a point α
$c = 1, \dots, C$	Clusters
$\mathbf{z} \in \{1, \dots, C\}^K$	Cluster assignments
$\mu_c \in \Delta^M$	Cluster centers
ρ	Subregion radius

models $\{g_k^*\}_{k=0}^K$, i.e.,

$$g_0^* = \operatorname{argmin}_{g_0} F^*(g_0) \equiv \sum_{k=1}^K p(k) F_k^*(g_0), \quad (1)$$

$$g_k^* = \operatorname{argmin}_{g_k} F_k^*(g_k) \text{ for } k = 1, \dots, K, \quad (2)$$

$$\text{where } F_k^*(g) = \mathbb{E}_{(\mathbf{x}, y) \sim p_k(\mathbf{x}, y)} [f(g, (\mathbf{x}, y))].$$

Here, $p(k)$ is the normalized population of data samples over the clients, $p_k(\mathbf{x}, y)$ is the data distribution for the client k , and $f(g, (\mathbf{x}, y))$ is the loss, e.g., cross-entropy, of the model g on a sample $(\mathbf{x}, y) \in \mathbb{R}^{I \times L}$, where I is the dimension of an input data sample. *Global* (Zhang et al., 2021) and *personalized* (Tan et al., 2022) FL aim to approximate g_0^* and $\{g_k^*\}_{k=1}^K$, respectively, by using the training data $\mathcal{D} = \{\mathcal{D}_k\}_{k=1}^K$ observed by the clients. Throughout the paper, we assume that all models are neural networks (NNs) $\hat{y} = g_k(\mathbf{x}; \mathbf{w}_k)$ with the same architecture, and represent the model g_k with its NN weight parameters $\mathbf{w}_k \in \mathbb{R}^D$, i.e., we hereafter represent $g_k(\mathbf{x}; \mathbf{w}_k)$ by \mathbf{w}_k and thus denote, e.g., $F_k^*(g_k)$ by $F_k^*(\mathbf{w}_k)$. Let $N = \sum_{k=1}^K N_k$, $N_k = |\mathcal{D}_k|$.

For the independent and identically distributed (IID) data setting, i.e., $p_k(x, y) = p(x, y), \forall k = 1, \dots, K$, the global and personalized FL aim for the same goal, and the minimum loss solution for the given training data is

$$\hat{\mathbf{w}}_0 = \hat{\mathbf{w}}_k = \operatorname{argmin}_{\mathbf{w}} F(\mathbf{w}) \equiv \sum_{k=1}^K \frac{N_k}{N} F_k(\mathbf{w}), \quad (3)$$

$$\text{where } F_k(\mathbf{w}) = \frac{1}{N_k} \sum_{(\mathbf{x}, y) \in \mathcal{D}_k} f(\mathbf{w}, (\mathbf{x}, y)).$$

In this setting, Federated Averaging (FedAvg) (McMahan et al., 2017),

$$\mathbf{w}_0^{t+1} = \mathbf{w}_0^t + \sum_{k \in \mathcal{S}^t} \frac{N_k}{N} \cdot \Delta \mathbf{w}_k^{t+1} \text{ for } t = 1, \dots, T, \quad (4)$$

is known to converge to $\widehat{\mathbf{w}}_0$, and thus solve Eq. (3). Here, \mathcal{S}^t is the set of clients that participate the t -th communication round, and $\Delta \mathbf{w}_k^{t+1} = \mathbf{w}_k^{t+1} - \mathbf{w}_0^t$ is the update after T' steps of the local gradient descent,

$$\check{\mathbf{w}}^{t'+1} = \check{\mathbf{w}}^{t'} - \gamma \nabla F_k(\check{\mathbf{w}}^{t'}), \text{ for } t' = 1, \dots, T', \quad (5)$$

where $\check{\mathbf{w}}^0 = \mathbf{w}_0^t$, $\check{\mathbf{w}}^{T'} = \mathbf{w}_k^{t+1}$, and γ is the step size. FedAvg has been further enhanced with, e.g., proximity regularization (Li et al., 2020), auxiliary data (Sattler et al., 2023), and ensembling (Shi et al., 2021).

On the other hand, in the more realistic non-IID setting, where $\mathbf{w}_0^* \neq \mathbf{w}_k^*$, FedAvg and its variants suffer from slow convergence and poor performance (Zhu et al., 2021). To address such challenges, Ditto (Li et al., 2021) was proposed for personalized FL, i.e., to approximate the best local models $\{\mathbf{w}_k^*\}_{k=1}^K$. Ditto has two training phases: it first trains the global model $\widehat{\mathbf{w}}_0$ by FedAvg, then trains the local models with proximity regularization to $\widehat{\mathbf{w}}_0$, i.e.,

$$\widehat{\mathbf{w}}_k = \operatorname{argmin}_{\mathbf{w}_k} \widetilde{F}_k(\mathbf{w}_k, \widehat{\mathbf{w}}_0) \equiv F_k(\mathbf{w}_k) + \frac{\lambda}{2} \|\mathbf{w}_k - \widehat{\mathbf{w}}_0\|_2^2,$$

where λ controls the divergence from the global model.

Ditto outperforms other non-IID FL methods, including the client clustering method HYPCLUSTER, adaptive federated learning (APFL), which interpolates between a global and local models (Deng et al., 2020), Loopless Local SGD (L2SGD), which applies global and local model average regularization (Hanzely & Richtarik, 2021), and MOCHA (Smith et al., 2017), which fits task-specific models through a multi-task objective. We refer readers to Tan et al. (2022) for a comprehensive study of existing personalized FL methods.

2.2. Mode Connectivity and Solution Simplex

Daniel Freeman & Bruna (2017), as well as Garipov et al. (2018), discovered the mode connectivity in the NN parameter space—the existence of simple paths with low training loss between two well-trained models from different initializations. Nagarajan & Kolter (2019) showed that the path is linear when the models are trained from the same initialization, but with different ordering of training data. Frankle et al. (2020) showed that the same pre-trained models stay linearly-connected after fine-tuning with gradient noise or different data ordering.

Benton et al. (2021) found that the low loss connection is not necessarily in 1D, and Wortsman et al. (2021) showed

that a simplex,

$$\mathcal{W}(\{\boldsymbol{\theta}_m\}) = \left\{ \mathbf{w}_\alpha(\{\boldsymbol{\theta}_m\}) = \sum_{m=1}^{M+1} \alpha_m \boldsymbol{\theta}_m; \boldsymbol{\alpha} \in \Delta^M \right\}, \quad (6)$$

within which any point has a small loss, can be trained from randomly initialized endpoints. Here, $\{\boldsymbol{\theta}_m \in \mathbb{R}^D\}_{m=1}^{M+1}$ are the endpoints or vertices of the simplex, and $\Delta^M = \{\boldsymbol{\alpha} \in [0, 1]^{M+1}; \|\boldsymbol{\alpha}\|_1 = 1\}$ denotes the M -dimensional standard simplex. This simplex learning is performed by finding the endpoints that (approximately) minimize

$$\mathbb{E}_{(\mathbf{x}, y) \sim p(\mathbf{x}, y)} \left[\mathbb{E}_{\mathbf{w} \sim \mathcal{U}_{\mathcal{W}(\{\boldsymbol{\theta}_m\})}} [f(\mathbf{w}, (\mathbf{x}, y))] \right], \quad (7)$$

where $\mathcal{U}_{\mathcal{W}}$ denotes the uniform distribution on a set \mathcal{W} .

3. Proposed Method

3.1. Problem Setting

In this paper, we assume the covariate shift non-IID scenario, where the input-output relation $p_k(y|\mathbf{x}) = p(y|\mathbf{x})$, $\forall k = 1, \dots, K$ is common over the clients, while the input distributions can be diverse, i.e., $p_k(\mathbf{x}) \neq p_{k'}(\mathbf{x})$ for some pairs k, k' . We furthermore assume that the server has access to the information on the output distributions $p_k(y) = \int p(y|\mathbf{x}) p_k(\mathbf{x}) d\mathbf{x}$ of the clients. Unless the privacy preservation can be compromised, e.g., when FL is applied for coping with constrained communication channels (Chen et al., 2022a; So et al., 2022), or for complying with data ownership, intellectual property, and regulation policies (European Commission, 2016), privacy-aware sharing should be performed, e.g., through trusted execution environments (Bhope et al., 2023) or by utilizing approximation methods based on the client’s weights (Ramakrishna & Dán, 2022) or public data sets (Wang et al., 2021).

3.2. SosisicFL Overview

The main idea behind SosisicFL is to share the solution simplex (6) with the clients in a way that similar clients behave similarly with systematic regularization. Specifically, in its preparation stage, SosisicFL clusters the clients based on the client label distributions $\{p_k(y)\}_{k=1}^K$, and assigns each cluster a subregion in the standard simplex for $\boldsymbol{\alpha} \in \Delta^M$ (Section 3.3). Let $\mathbf{z} \in \{1, \dots, C\}^K$ be the cluster assignment of the clients, i.e., the client k belongs to the cluster z_k , and $\mathcal{R}_c \subseteq \Delta^M$ be the subregion assigned to the cluster c . The server and the client k share the information on the assigned subregion \mathcal{R}_{z_k} .

FL starts from randomly initialized simplex endpoints $\{\boldsymbol{\theta}_m\}_{m=1}^{M+1}$, and performs the following steps for each participating client $k \in \mathcal{S}^t$ in each communication round t :

1. The master sends the current endpoints $\{\boldsymbol{\theta}_m^t\}_{m=1}^{M+1}$ to the client k .

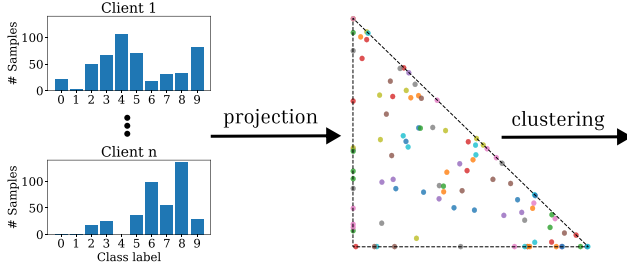


Figure 2. Client clustering and subregion assignment process. Based on the label distributions (left-most), we project clients onto a simplex and cluster them.

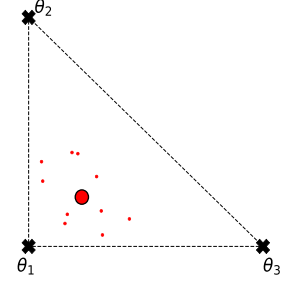


Figure 3. During training, each client samples α from the uniform distribution on the subregion \mathcal{R}_{z_k} that was assigned to the cluster it belongs to.

2. The client k performs simplex learning only on $\mathcal{U}_{\mathcal{R}_{z_k}}$ as a local update. Namely, in each local gradient descent update t' , it draws a sample $\alpha \sim \mathcal{U}_{\mathcal{R}_{z_k}}$, computes the loss of the corresponding model $w_\alpha = \sum_{m=1}^{M+1} \alpha_m \theta_m^t$, and updates the endpoints (Section 3.4).
3. The client sends the local update of the endpoints to the master.

This way, SosisFL is expected to learn the global solution simplex $\{w_\alpha; \alpha \in \Delta^M\}$, while allowing divergence of the local clients distributed within the solution simplex. Algorithm 1 shows the main steps. Below, we give details of client clustering, the preparation step, the communication round, and inference.

3.3. Preparation Stage: Client Clustering and Subregion Assignment

This preparation step aims to assign subregions of the solution simplex (6) to the groups, i.e., clusters, of clients. This can be done in the standard simplex for $\alpha \in \Delta^M$ independently from the endpoints $\{\theta_m\}_{m=1}^{M+1}$. We assume that the client label distributions $\{p_k(y)\}_{k=1}^K$ are given as the multinomial parameters $\Phi = (\phi_1, \dots, \phi_K) \in (\Delta^{L-1})^K \subset \mathbb{R}^{L \times K}$ as $p_k(y=l) = \Phi_{l,k}$. Seeing the multinomial parameters as feature vectors, we first project $\phi_k \in \Delta^{L-1}$ onto the lower-dimensional simplex $\alpha_k(\phi_k) \in \Delta^M$ (assuming $L-1 > M$). We perform this dimensionality reduction by Latent Dirichlet Allocation (LDA) (Blei et al., 2003). LDA is a Bayesian model with mixtures of multinomial distributions, where the “word” distribution of each “document” is expressed as a mixture of the word distributions of “topics,” providing the topic distribution of each document as a low-dimensional representation. In our case, the documents and the words correspond to the clients and the labels, respectively, and LDA thus provides α_k as the mixing weights over the $M+1$ topics. We use an implementation of the

Algorithm 1 SosisFL

- 1: **Input:** Learning rate γ , number of communication rounds T , number of clients K , number of selected clients per round $|\mathcal{S}^t|$, number of local epochs E , simplex dimension M , number of clusters C , subregion size ρ .
 - 2: **Initialize:** solution simplex (endpoints) $\{\theta_m^0\}_{m=1}^{M+1}$.
Get label distributions:
 - 3: $\{\phi_k\}_{k=1}^K \leftarrow \text{Collect_Client_Label_Distributions}()$
Get cluster regions $\{\mathcal{R}_c\}_{c \in C}$ with LDA model Λ and HSC:
 - 4: $\{\mathcal{R}_c\}_{c=1}^C \leftarrow \text{Client_Clustering}(\{\phi_k\}_{k=1}^K, M)$
 - 5: **for** $t = 1$ **to** T **do**
 - 6: **for** $k \in \mathcal{S}_t$ **do**
 - 7: $\{\theta_{m,k}^{t+1}\}_{m=1}^{M+1} \leftarrow \text{Local_Update}(\{\theta_{m,k}^t\}_{m=1}^{M+1})$
 - 8: **end for**
 - 9: $\{\theta_m^{t+1}\}_{m=1}^{M+1} \leftarrow \text{Global_Update}(\{\{\theta_{m,k}^{t+1}\}_{m=1}^{M+1}\}_{k \in \mathcal{S}^t})$
 - 10: **end for**
-

online variational Bayes algorithm (Hoffman et al., 2010).

We then cluster the client representations $\{\alpha_k\}_{k=1}^K$ into C groups by Hilbert simplex clustering (HSC) (Nielsen & Sun, 2019), a theoretically-grounded and computationally-friendly algorithm for clustering in a simplex, with the L1-distance, providing the cluster assignments $z \in \{1, \dots, C\}^K$ and cluster centers $\{\mu_c\}_{c=1}^C$. For each cluster, we assign a subregion $\mathcal{R}_c = \mathcal{B}_\eta(\mu_c)$, where $\mathcal{B}_{q,\eta}(\mu) = \{x \in \Delta^M; \|x - \mu\|_q \leq \eta\}$ denotes the L_q -distance η -ball around μ . Figure 2 illustrates the preparation procedure, which determines the subregion \mathcal{R}_{z_k} assigned to each client k . We set the radius of the ball to $\eta = \rho \bar{\delta}$, where ρ is the parameter controlling the overlap between the cluster subregions, and $\bar{\delta} = \frac{1}{C} \sum_{c=1}^C \frac{\int_{\Delta^M} \|\mu_c - \alpha'\|_1 d\alpha'}{\int_{\Delta^M} d\alpha'}$ is the average distance from all clusters to all points within the simplex, which is approximated by the grid integration.

3.4. Communication Round: Local and Global Updates

In the t -th communication round, the master sends the current endpoints $\{\theta_m^t\}_{m=1}^{M+1}$ to the participating clients \mathcal{S}^t . Then, each client $k \in \mathcal{S}^t$ draws Ω_{tr} random samples from the uniform distribution $\mathcal{A} = \{\alpha^i\}_{i=1}^{\Omega_{tr}} \sim \mathcal{U}_{\mathcal{R}_{z_k}}$ on the assigned subregion (see Fig. 3), and applies T' local updates,

$$\check{\theta}_m^{t'+1} = \check{\theta}_m^{t'} - \alpha_m \cdot \gamma \cdot \nabla F_k(\mathbf{w}_\alpha), \quad (8)$$

to the endpoints with α sequentially chosen from \mathcal{A} . Here $\check{\theta}_m^0 = \theta_m^t$, $\check{\theta}_m^{T'} = \theta_m^{t+1}$. The local updates $\{\Delta\theta_{m,k}^{t+1} = \theta_{m,k}^{t+1} - \theta_m^t\}_{m=1}^{M+1}$ are sent back to the master, which updates the endpoints as

$$\theta_m^{t+1} = \theta_m^t + \sum_{k \in \mathcal{S}^t} \frac{N_k}{N} \cdot \Delta\theta_{m,k}^{t+1}. \quad (9)$$

3.5. Inference

With the trained endpoints $\{\hat{\theta}_m = \theta_m^T\}_{m=1}^{M+1}$, we simply use $\mathbf{w}_{\hat{\alpha}_0}(\{\hat{\theta}_m\}_{m=1}^{M+1})$ and $\{\mathbf{w}_{\hat{\alpha}_k}(\{\hat{\theta}_m\}_{m=1}^{M+1})\}_{k=1}^K$ as the global and local models, where

$$\hat{\alpha}_0 = \frac{1}{M+1} \mathbf{1}_{M+1}, \quad \hat{\alpha}_k = \boldsymbol{\mu}_{z_k},$$

with $\mathbf{1}_D$ denoting the D -dimensional all one vector.

3.6. Variants

SosicFL and SosicFL-All Simplex training is not necessarily applied to all NN parameters. In preliminary experiments, we found that simplex learning applied only to the last fully connected layer, i.e., the classification head, is effective—it accelerates training without significant performance drop (see Appendix B for empirical results). We set this version as the default SosicFL, and call the version where simplex learning is applied to all NN parameters SosicFL-all. SosicFL can be applied to pre-trained models, which is highly beneficial because it was shown that starting from pretrained models can significantly accelerate FL, closing the gap between IID and non-IID settings (Chen et al., 2022b; Nguyen et al., 2022).

SosicFL⁺ We can enhance the personalized FL performance of SosicFL by applying Ditto (Li et al., 2021) after SosicFL training. In this version, called SosicFL⁺, each client personalizes the global endpoints $\{\hat{\theta}_m^0 = \theta_m\}_{m=1}^{M+1}$ by local gradient descent to minimize the Ditto objective, i.e.,

$$\begin{aligned} \{\hat{\theta}_m^k\} &= \operatorname{argmin}_{\{\theta_m\}} \tilde{F}_k(\{\theta_m\}, \{\hat{\theta}_m^0\}) \\ &\equiv \mathbb{E}_{\alpha \sim \mathcal{U}_{\mathcal{R}_{z_k}}} [F_k(\mathbf{w}_\alpha(\{\theta_m\}))] + \frac{\lambda}{2} \sum_{m=1}^{M+1} \|\theta_m - \hat{\theta}_m^0\|_2^2. \end{aligned}$$

4. Experiments

4.1. Experimental Setup

Models and data sets. To evaluate SosicFL, we perform image classification on the CIFAR-10 (Krizhevsky et al., 2009) and Tiny-ImageNet (Deng et al., 2009) datasets. For CIFAR-10, we train a simple CNN (Hahn et al., 2022) from scratch, as well as a SqueezeNet (Iandola et al., 2016) that has been pre-trained on ImageNet (Deng et al., 2009) before we fine-tune it, as proposed in Nguyen et al. (2022). For Tiny-ImageNet, we train a MobileNetV2 (Sandler et al., 2018) from scratch as proposed in Shi et al. (2023) as well as a ResNet18 (He et al., 2016) pre-trained on ImageNet before we fine-tune it as in Chen et al. (2022b). We provide a table with all hyperparameters that we use for each data set/model setting in Appendix A.

Data heterogeneity. To simulate heterogeneous clients, we implement two partitioning procedures. The first procedure by Huang et al. (2021) partitions clients in equally sized groups and assigns each group a set of primary classes. Every client gets $z\%$ of its data from its group’s primary classes and $(100 - z)\%$ from the remaining classes. We apply this method with $x = 80$ for two and five groups and refer to these splits as *2-Fold* and *5-Fold*. For example, in CIFAR-10 *2-Fold*, half of the clients get assigned 80% samples from classes 1-5 and 20% from classes 6-10.

The second procedure, inspired by Yurochkin et al. (2019) and Gao et al. (2022), draws the multinomial parameters of the client distributions $p_k(y) = \text{Multi}(y; \phi_k)$ from Dirichlet, i.e., $\phi_k \sim \text{Dir}_L(\beta)$, where β is the concentration parameter controlling the sparsity and heterogeneity— $\beta \rightarrow \infty$ concentrates the mass to the uniform distribution (and thus homogeneous), while small $0 < \beta < 1$ generates sparse and heterogeneous non-IID client distributions.

Baselines. We choose FedAvg (McMahan et al., 2017), FedProx (Li et al., 2020), and Ditto (Li et al., 2021) as the baseline methods. The last two are the state-of-the-art for global FL and personalized FL, respectively.

Parameter setting. For all SosicFL-based methods, we set the number of clusters to $C = 10$ in the Dirichlet setting and to $C = 2, 5$ in the *2-Fold* and *5-Fold* settings, respectively. We set the subregion radius parameter to $\rho = 0.6$ for *2-Fold* experiments and $\rho = 0.4$ for all other experiments. We found those settings work well in our preliminary experiments, and conducted ablation study with other parameter settings in Section 4.3. For the baselines, we follow the recommended parameter settings by the authors, which are detailed in Appendix A.

Table 2. Average *global* and *local* test accuracy on randomly initialized models.

	CIFAR-10 on SimpleCNN						TinyImagenet on MobileNet V2					
	2-Fold		5-Fold		Dir(0.5)		2-Fold		5-Fold		Dir(0.3)	
FedAvg	68.97	68.90	66.76	66.82	68.75	69.13	10.10	28.17	9.51	27.45	19.02	19.29
FedProx	68.73	68.84	66.67	66.70	68.68	69.14	9.77	28.06	9.61	27.49	19.04	19.39
SosicFL	70.35	75.74	67.54	71.37	69.39	71.24	11.02	32.39	9.89	31.16	20.41	21.31
Ditto			66.50	79.95	68.40	74.87			9.74	30.94	18.89	22.69
SosicFL ⁺			67.83	80.67	69.83	75.88			10.01	33.88	21.18	24.81

 Table 3. Average *global* and *local* test accuracy on pre-trained models.

	CIFAR-10 on SqueezeNet						TinyImagenet on ResNet18					
	2-Fold		5-Fold		Dir(0.1)		2-Fold		5-Fold		Dir(0.3)	
FedAvg	58.69	58.56	53.78	52.51	48.58	48.46	43.46	54.69	40.71	51.68	49.91	49.92
FedProx	59.76	59.28	29.81	27.89	50.08	50.62	43.14	54.66	40.34	51.59	50.04	49.99
SosicFL	63.32	71.67	60.34	67.86	54.63	63.72	44.05	60.91	41.68	59.56	50.95	51.11
Ditto			55.70	75.56	50.54	84.34			40.71	56.16	49.92	53.84
SosicFL ⁺			59.78	78.00	55.60	85.42			42.14	61.58	51.30	54.42

Evaluation metrics. We adopt two metrics, the (best) test accuracy (ACC) and the time-to-accuracy (TTA), each for evaluating the global and local FL performance. ACC is the test accuracy over T communication rounds, i.e., $ACC(T) = \max_t \frac{1}{N_{\text{test}}} \sum_{i=1}^{N_{\text{test}}} \mathbb{1}(y_i = g(\mathbf{x}_i; \hat{\mathbf{w}}^t))$, where $\mathbb{1}(\cdot)$ is the indicator function that equals to 1 if the event is true and 0 otherwise. TTA evaluates the number of communication rounds needed to achieve the baseline (FedAvg and Ditto in this paper) test accuracy, i.e., $ACC_{\text{FedAvg}}(T)$. We report TTA improvement, i.e. the TTA of the baseline, e.g. FedAvg, divided by the TTA of the benchmarked method, e.g. SosicFL.

4.2. Results

Tables 2 and 3 summarize the main experimental results, where SosicFL and SosicFL⁺ consistently outperform the baselines across the different experiments. The maximum global and local test accuracy, averaged over 5 trial runs, is shown in red and blue, respectively.

We group the methods into two groups—with (Ditto and SosicFL⁺) or without (FedAvg, FedProx, and SosicFL) additional personalization steps¹—and highlight the best method in each group in bold. Ditto and SosicFL⁺ are excluded from the evaluation on 2-Fold setting because the setting is too close to IID. The performance in terms of TTA improvement is reported in Table 5 in Appendix C. Below we explain each experiment in detail.

¹Note that these personalized approaches require additional computational resources on each client as they train two models.

One-dimensional solution simplex on 2-Fold. We start from the simplest case, where a ($M = 1$)-dimensional simplex, i.e., line segment, solution is learned on the CIFAR-10 2-Fold split using a pre-trained SqueezeNet. Figure 4 shows the progress of the global (left) and local (right) test accuracy, where we observe that our SosicFL outperforms the baselines by a large margin. Additionally, the small standard deviation over the 5 trials, depicted as shadows, as well as the smooth curve over the communication rounds of SosicFL, in comparison with those of baselines, imply that our systematic regularization through the solution simplex stabilizes the training dynamics significantly.

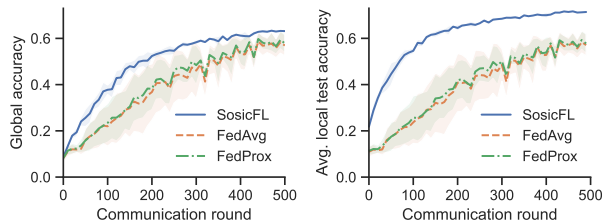


Figure 4. Global (left) and local (right) test accuracy on CIFAR-10 with 2-Fold setting and pre-trained SqueezeNet initialization.

Global and local FL performance. Next, we evaluate the global test performance on CIFAR-10 and TinyImageNet with the non-IID data splits generated by 2-Fold, 5-Fold, and Dir(β) procedures. Tables 2 and 3 show results of FL from random initialization and those from pre-trained models on ImageNet, respectively. We clearly see that our SosicFL and SosicFL⁺ outperform all baselines in each group.

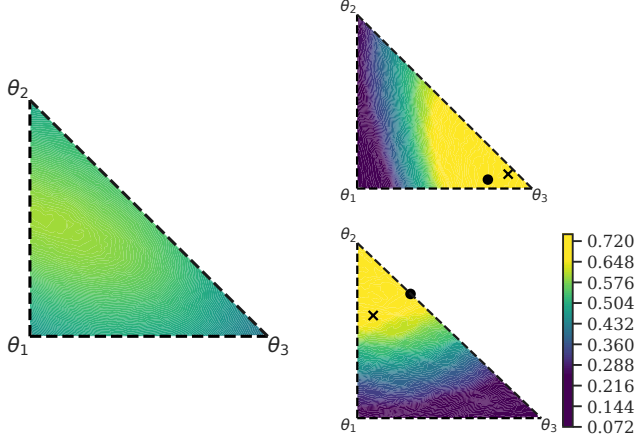


Figure 5. Global test accuracy (left) and local test accuracy of two clients (right). In SusicFL, clients use different subregions in the solution simplex to be personalized for their local distributions, while they collaboratively learn the accurate global simplex. On the right, \bullet marks the LDA representation of the corresponding client and \times marks the cluster center to which the client belongs.

4.3. Analysis and Discussion

Here, we further investigate the behavior of SusicFL to elucidate the mechanism of its good performance. All results in this subsection is of SusicFL on CIFAR-10 with the $\text{Dir}(0.1)$ non-IID split and SqueezeNet pre-trained initialization.

Solution structure in simplex. Here we investigate how the solution simplex is shared over clients. To this end, we draw 2000 uniformly distributed points in the solution simplex, and evaluate the global and the local test accuracy of the corresponding models. Figure 5 shows the global test accuracy (left) and the local test accuracy (right column) for two clients. As expected, the models around the assigned—through the cluster (center \times) it belongs to—subregions to the client (\bullet) show good local test accuracy for each client, while the models in the whole solution simplex show more uniform global performance. This result indicates that the heterogenous sharing of the solution simplex across the clients properly works as designed.

Gradient variance reduction. We observed in Figure 4 stable learning curves for SusicFL and SusicFL⁺ over communication rounds as well as trials. This implies that the degrees of freedom of the solution simplex could absorb the heterogeneity of clients to some extent, making the gradient signals homogeneous. To directly confirm this hypothesis, we plot in Figure 6 the total variance—the sum of the variances of the updates $\Delta \mathbf{w}_k^t = \mathbf{w}_k^t - \mathbf{w}_0^{t-1}$ for FedAvg and FedProx, and $\Delta \theta_{m,k}^t = \theta_{m,k}^t - \theta_{m,0}^{t-1}$ for SusicFL, respectively. More specifically, we compute the variance over the

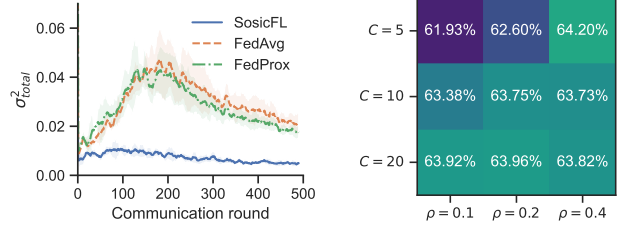


Figure 6. Total variance of the last fully-connected layer.

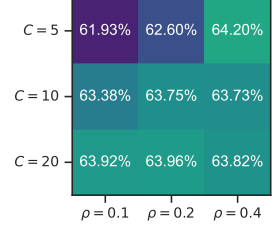


Figure 7. Local test accuracies for different numbers of clusters C and subregion radii ρ .

last fully-connected layer, given by

$$\sigma_{\text{total}}^2(t) = \sum_{k \in \mathcal{S}^t} \left\| \Delta \mathbf{w}_k^t - \frac{1}{|\mathcal{S}^t|} \sum_{k \in \mathcal{S}^t} \Delta \mathbf{w}_k^t \right\|_2^2, \quad (10)$$

for FedAvg and FedProx, and by

$$\sigma_{\text{total}}^2(t) = \sum_{k \in \mathcal{S}^t} \left\| \Delta \bar{\theta}_k^t - \frac{1}{|\mathcal{S}^t|} \sum_{k \in \mathcal{S}^t} \Delta \bar{\theta}_k^t \right\|_2^2, \quad (11)$$

with $\Delta \bar{\theta}_k^t = \frac{1}{M+1} \sum_{m=1}^{M+1} \Delta \theta_{m,k}^t$, for SusicFL. As discussed in Reddi et al. (2020); Karimireddy et al. (2020), a small total variance indicates effective collaborations with consistent gradient signals between the clients, leading to faster convergence and better performance. From the figure, we see that the total gradient of SusicFL is much lower and more stable than the baseline methods, which, together with its good performance observed in Tables 2 and 3, is consistent with their discussion. Moreover, Li et al. (2023) argued that the last classification layer has the biggest impact on performance, implying that reducing the total variance of the classification layer, as SusicFL does with simplex learning, is most effective.

Sensitivity to parameter setting. We investigate how stable the performance of SusicFL is for different parameter settings. Specifically, we tested SusicFL with the combination of $C = 5, 10, 20$ (number of clusters) and $\rho = 0.1, 0.2, 0.4$ (radius of subregions), and show the local accuracy in Figure 7. $C = 5, \rho = 0.4$ gives the best accuracy 64.20% (note that the results in Table 3 are with $C = 10, \rho = 0.4$, giving 63.73%, which is slightly worse than the optimal for this particular setting, i.e., CIFAR10, $\text{Dir}(0.1)$, SqueezeNet pre-trained initialization). More importantly, SusicFL with all these parameter choices outperforms the baseline, which indicates its good performance and weak sensitivity to the parameter setting.

Late start of subregion assignment. As mentioned in Section 3.1, SusicFL requires the client label distributions $\{p_k(y)\}$ to assign the subregion of the solution simplex. Here we consider the scenario where the the client distribution is not available at the beginning of FL, e.g., when

the client has no data in the beginning, but can send it to the master once the client observed a sufficient amount of data samples. Here, we evaluate the performance in this scenario. Assume that the client distributions are available only after the communication round \tilde{t} . Then, in the earlier rounds $t < \tilde{t}$, each client uses the whole simplex and draws $\alpha \in \Delta^M$ for the local update (8), which corresponds to a straightforward application of simplex learning to FedAvg. After clustering and subregion assignment are performed at $t = \tilde{t}$, the client starts using the assigned subregion, and performs the full SosisFL local updates. Figure 8 shows the local test accuracy of SosisFL for $\tilde{t} = 1, 250, \infty$. Note that $\tilde{t} = 1$ corresponds to the original scenario (where subregion assignment is ready from the beginning), and $\tilde{t} = \infty$ to the naive simplex learning with FedAvg. We observe that SosisFL($\tilde{t} = \infty$) slightly outperforms the baselines, which implies that the naive application of simplex learning gives moderate improvement. SosisFL($\tilde{t} = 250$) rapidly catches up with SosisFL($\tilde{t} = 1$) once the subregion assignment is done at $t = 250$, proving the usefulness of SosisFL in the late start scenario.

Computational complexity. If the batch size is one, simplex training adds $O(\pi \cdot M)$ computational complexity for each layer, where π is the parameter complexity of the layer, e.g., $\pi = d \cdot L$ for a fully connected layer with d input and L output neurons, and M is the simplex dimension (Wortman et al., 2021). For SosisFL, this additional complexity only applies to the classification layer. For inference, no additional complexity arises, compared to FedAvg, because inference is performed by the single model corresponding to the cluster center.

Since the most modern architectures, e.g., ResNet18 and Vision Transformer (ViT) (Dosovitskiy et al., 2021), have parameter complexity of $O(\mathbb{G}_{\text{FE}}) \gg O(\mathbb{G}_{\text{C}})$, where \mathbb{G}_{FE} and \mathbb{G}_{C} are the complexities of the feature extractor and the classification layer, respectively, the additional training complexity, applied only to the classification layer, of SosisFL is ignorable, i.e., $O(\mathbb{G}_{\text{FE}}) \gg O(\mathbb{G}_{\text{C}} \cdot M)$. The same applies to the communication costs: since the simplex

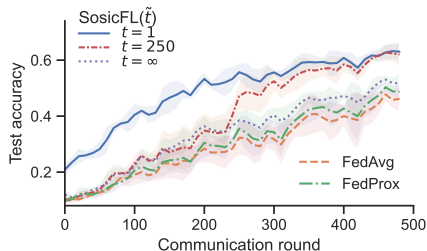


Figure 8. Average local test accuracy when clustering the solution simplex at different communication rounds t .

learning is applied only to the classification layer, the increase of communication costs are ignorable compared to the communication costs for the feature extractor.

5. Related Work

There are a few methods that apply simplex learning to federated learning. Hahn et al. (2022) showed that enforcing a low loss simplex between independently initialized global and client models yields good personalized FL performance. Their approach builds on previous related work which finds optimal interpolation coefficients between a global and local model (Deng et al., 2020) to improve personalized FL. However, their simplex is restricted to be 1D, i.e., a line segment, and the global model performance is comparable to the plain FedAvg. Moreover, they train a solution simplex over all layers between global and local models, which is computationally expensive and limits its applicability to training *from scratch*. This should be avoided if pre-trained models are available (Nguyen et al., 2022; Chen et al., 2022b). Lastly, they do not employ clustering of any sort. Our method generalizes to training low loss simplices of higher dimensions in a FL setting, tackles both the global and personalized FL objectives, is applicable to pre-trained models, and shows significant performance gains by employing clustering based on local client data.

6. Conclusion

Federated learning (FL) with highly non-IID client data distributions is still a challenging problem and a very actively researched topic. Recent works tackle non-IID FL settings either through global or personalized FL. While the former aims to find a single optimal set of parameters that fit a global objective, the latter tries to optimize multiple local models each of which fits the local distributions well. These two different objectives may pose a trade-off, that is, personalized FL might adapt models to strongly to local distributions which might harm the global performance, while global FL solutions might fit none of the local distributions if the local distributions are diverse. In this paper, we have tackled to solve this dilemma. Specifically, we propose SosisFL, which assigns subregions of the solution simplex to the clients so that they have flexibility for personalization, and at the same, contribute to learning the global solution simplex. SosisFL shows state-of-the-art performance both in global and personalized FL with minimal computational and communication overhead at training and no overhead at inference. Furthermore, we showed the applicability of SosisFL to pre-trained models, which is not possible for the methods that learn the solution simplex in the whole network parameter space.

Promising future research directions include better under-

standing the decision-making process of solution simplex training through global and local explainable AI methods (Bach et al., 2015; Samek et al., 2021; Bykov et al., 2023). Furthermore, we want to apply our approach to continual learning problems and FL scenarios with highly varying client availability (Rodio et al., 2023; Wiesner et al., 2024).

7. Acknowledgements

This work was funded by the German Ministry for Education and Research as BIFOLD - Berlin Institute for the Foundations of Learning and Data (ref. BIFOLD23B).

8. Impact Statement

This paper presents work whose goal is to advance the field of Machine Learning. There are many potential societal consequences of our work, none which we feel must be specifically highlighted here.

References

- Bach, S., Binder, A., Montavon, G., Klauschen, F., Müller, K.-R., and Samek, W. On pixel-wise explanations for non-linear classifier decisions by layer-wise relevance propagation. *PLOS ONE*, 10(7):1–46, 07 2015.
- Benton, G., Maddox, W., Lotfi, S., and Wilson, A. G. G. Loss surface simplexes for mode connecting volumes and fast ensembling. In *International Conference on Machine Learning*, pp. 769–779. PMLR, 2021.
- Bhope, R. A., Jayaram, K. R., Venkatasubramanian, N., Verma, A., and Thomas, G. Flips: Federated learning using intelligent participant selection. In *International Middleware Conference*, pp. 301–315. ACM, 2023.
- Blei, D. M., Ng, A. Y., and Jordan, M. I. Latent dirichlet allocation. *Journal of Machine Learning Research*, 3 (Jan):993–1022, 2003.
- Bykov, K., Deb, M., Grinwald, D., Müller, K.-R., and Höhne, M. M.-C. Dora: Exploring outlier representations in deep neural networks. *Transactions on Machine Learning Research*, 2023. ISSN 2835-8856.
- Chen, H., Huang, S., Zhang, D., Xiao, M., Skoglund, M., and Poor, H. V. Federated learning over wireless iot networks with optimized communication and resources. *IEEE Internet of Things Journal*, 9(17):16592–16605, 2022a.
- Chen, H.-Y., Tu, C.-H., Li, Z., Shen, H. W., and Chao, W.-L. On the importance and applicability of pre-training for federated learning. In *International Conference on Learning Representations*, 2022b.
- Daniel Freeman, C. and Bruna, J. Topology and geometry of half-rectified network optimization. In *International Conference on Learning Representations*, 2017.
- Deng, J., Dong, W., Socher, R., Li, L.-J., Li, K., and Fei-Fei, L. Imagenet: A large-scale hierarchical image database. In *IEEE/CVF Conference on Computer Vision and Pattern Recognition*, pp. 248–255. Ieee, 2009.
- Deng, Y., Kamani, M. M., and Mahdavi, M. Adaptive personalized federated learning. *arXiv preprint arXiv:2003.13461*, 2020.
- Dosovitskiy, A., Beyer, L., Kolesnikov, A., Weissenborn, D., Zhai, X., Unterthiner, T., Dehghani, M., Minderer, M., Heigold, G., Gelly, S., Uszkoreit, J., and Houlsby, N. An image is worth 16x16 words: Transformers for image recognition at scale. In *International Conference on Learning Representations*, 2021.
- Draxler, F., Veschgini, K., Salmhofer, M., and Hamprecht, F. Essentially no barriers in neural network energy landscape. In *International conference on machine learning*, pp. 1309–1318. PMLR, 2018.
- European Commission. Regulation (EU) 2016/679 of the European Parliament and of the Council of 27 April 2016 on the protection of natural persons with regard to the processing of personal data and on the free movement of such data, and repealing Directive 95/46/EC (General Data Protection Regulation), 2016.
- Frankle, J., Dziugaite, G. K., Roy, D., and Carbin, M. Linear mode connectivity and the lottery ticket hypothesis. In *International Conference on Machine Learning*, pp. 3259–3269. PMLR, 2020.
- Gao, L., Fu, H., Li, L., Chen, Y., Xu, M., and Xu, C.-Z. Feddc: Federated learning with non-iid data via local drift decoupling and correction. In *IEEE/CVF Conference on Computer Vision and Pattern Recognition*, 2022.
- Garipov, T., Izmailov, P., Podoprikin, D., Vetrov, D. P., and Wilson, A. G. Loss surfaces, mode connectivity, and fast ensembling of dnns. *Advances in Neural Information Processing Systems*, 31, 2018.
- Hahn, S.-J., Jeong, M., and Lee, J. Connecting low-loss subspace for personalized federated learning. In *ACM SIGKDD Conference on Knowledge Discovery and Data Mining*, pp. 505–515, 2022.
- Hanzely, F. and Richtarik, P. Federated learning of a mixture of global and local models, 2021.
- He, K., Zhang, X., Ren, S., and Sun, J. Deep residual learning for image recognition. In *IEEE/CVF Conference on Computer Vision and Pattern Recognition*, pp. 770–778, 2016.

- Hoffman, M., Bach, F., and Blei, D. Online learning for latent dirichlet allocation. *Advances in Neural Information Processing Systems*, 23, 2010.
- Huang, Y., Chu, L., Zhou, Z., Wang, L., Liu, J., Pei, J., and Zhang, Y. Personalized cross-silo federated learning on non-iid data. In *AAAI conference on artificial intelligence*, volume 35, pp. 7865–7873, 2021.
- Iandola, F. N., Han, S., Moskewicz, M. W., Ashraf, K., Dally, W. J., and Keutzer, K. Squeezenet: Alexnet-level accuracy with 50x fewer parameters and 0.5 mb model size. *arXiv preprint arXiv:1602.07360*, 2016.
- Karimireddy, S. P., Kale, S., Mohri, M., Reddi, S., Stich, S., and Suresh, A. T. Scaffold: Stochastic controlled averaging for federated learning. In *International conference on machine learning*, pp. 5132–5143. PMLR, 2020.
- Krizhevsky, A., Hinton, G., et al. Learning multiple layers of features from tiny images. Technical report, 2009.
- Kulkarni, V., Kulkarni, M., and Pant, A. Survey of personalization techniques for federated learning. In *2020 Fourth World Conference on Smart Trends in Systems, Security and Sustainability (WorldS4)*, pp. 794–797. IEEE, 2020.
- Lai, F., Zhu, X., Madhyastha, H. V., and Chowdhury, M. Oort: Efficient federated learning via guided participant selection. In *15th {USENIX} Symposium on Operating Systems Design and Implementation ({OSDI} 21)*, pp. 19–35, 2021.
- Li, B., Schmidt, M. N., Alstrøm, T. S., and Stich, S. U. On the effectiveness of partial variance reduction in federated learning with heterogeneous data. In *IEEE/CVF Conference on Computer Vision and Pattern Recognition*, pp. 3964–3973, 2023.
- Li, T., Sahu, A. K., Zaheer, M., Sanjabi, M., Talwalkar, A., and Smith, V. Federated optimization in heterogeneous networks. *Machine Learning and Systems*, 2:429–450, 2020.
- Li, T., Hu, S., Beirami, A., and Smith, V. Ditto: Fair and robust federated learning through personalization. In *International Conference on Machine Learning*, pp. 6357–6368. PMLR, 2021.
- McMahan, B., Moore, E., Ramage, D., Hampson, S., and y Arcas, B. A. Communication-efficient learning of deep networks from decentralized data. In *Artificial intelligence and statistics*, pp. 1273–1282. PMLR, 2017.
- Mirzadeh, S. I., Farajtabar, M., Gorur, D., Pascanu, R., and Ghasemzadeh, H. Linear mode connectivity in multitask and continual learning. *arXiv preprint arXiv:2010.04495*, 2020.
- Nagarajan, V. and Kolter, J. Z. Uniform convergence may be unable to explain generalization in deep learning. *Advances in Neural Information Processing Systems*, 32, 2019.
- Nguyen, J., Wang, J., Malik, K., Sanjabi, M., and Rabat, M. Where to begin? on the impact of pre-training and initialization in federated learning. *arXiv preprint arXiv:2210.08090*, 2022.
- Nielsen, F. and Sun, K. *Clustering in Hilbert’s Projective Geometry: The Case Studies of the Probability Simplex and the Elliptope of Correlation Matrices*, pp. 297–331. Springer, 2019.
- Pillutla, K., Kakade, S. M., and Harchaoui, Z. Robust aggregation for federated learning. *IEEE Transactions on Signal Processing*, 70:1142–1154, 2022.
- Ramakrishna, R. and Dán, G. Inferring class-label distribution in federated learning. In *ACM Workshop on Artificial Intelligence and Security*, pp. 45–56, 2022.
- Reddi, S., Charles, Z., Zaheer, M., Garrett, Z., Rush, K., Konečný, J., Kumar, S., and McMahan, H. B. Adaptive federated optimization. *arXiv preprint arXiv:2003.00295*, 2020.
- Rodio, A., Faticanti, F., Marfoq, O., Neglia, G., and Leonardi, E. Federated learning under heterogeneous and correlated client availability. In *IEEE International Conference on Computer Communications*, 2023.
- Samek, W., Montavon, G., Lapuschkin, S., Anders, C. J., and Müller, K.-R. Explaining deep neural networks and beyond: A review of methods and applications. *Proceedings of the IEEE*, 109(3):247–278, 2021.
- Sandler, M., Howard, A., Zhu, M., Zhmoginov, A., and Chen, L.-C. Mobilenetv2: Inverted residuals and linear bottlenecks. In *IEEE/CVF Conference on Computer Vision and Pattern Recognition*, pp. 4510–4520, 2018.
- Sattler, F., Müller, K.-R., and Samek, W. Clustered federated learning: Model-agnostic distributed multitask optimization under privacy constraints. *IEEE Transactions on Neural Networks and Learning Systems*, 32(8):3710–3722, 2020.
- Sattler, F., Korjakow, T., Rischke, R., and Samek, W. Fedaux: Leveraging unlabeled auxiliary data in federated learning. *IEEE Transactions on Neural Networks and Learning Systems*, 34(9):5531–5543, 2023.
- Shi, N., Lai, F., Kontar, R. A., and Chowdhury, M. Fed-ensemble: Improving generalization through model ensembling in federated learning. *arXiv preprint arXiv:2107.10663*, 2021.

- Shi, Y., Liang, J., Zhang, W., Xue, C., Tan, V. Y. F., and Bai, S. Understanding and mitigating dimensional collapse in federated learning. *IEEE Transactions on Pattern Analysis and Machine Intelligence*, pp. 1–14, 2023.
- Smith, V., Chiang, C.-K., Sanjabi, M., and Talwalkar, A. S. Federated multi-task learning. *Advances in Neural Information Processing Systems*, 30, 2017.
- So, J., Hsieh, K., Arzani, B., Noghabi, S., Avestimehr, S., and Chandra, R. Fedspace: An efficient federated learning framework at satellites and ground stations. *arXiv preprint arXiv:2202.01267*, 2022.
- Tan, A. Z., Yu, H., Cui, L., and Yang, Q. Towards personalized federated learning. *IEEE Transactions on Neural Networks and Learning Systems*, 2022.
- Wang, L., Xu, S., Wang, X., and Zhu, Q. Addressing class imbalance in federated learning. In *AAAI Conference on Artificial Intelligence*, volume 35, pp. 10165–10173, 2021.
- Wiesner, P., Khalili, R., Grinwald, D., Agrawal, P., Thamsen, L., and Kao, O. Fedzero: Leveraging renewable excess energy in federated learning. In *International Conference on Future and Sustainable Energy Systems*. ACM, 2024.
- Wortsman, M., Horton, M. C., Guestrin, C., Farhadi, A., and Rastegari, M. Learning neural network subspaces. In *International Conference on Machine Learning*, pp. 11217–11227. PMLR, 2021.
- Yurochkin, M., Agarwal, M., Ghosh, S., Greenewald, K., Hoang, N., and Khazaeni, Y. Bayesian nonparametric federated learning of neural networks. In *International conference on machine learning*, pp. 7252–7261. PMLR, 2019.
- Zhang, C., Xie, Y., Bai, H., Yu, B., Li, W., and Gao, Y. A survey on federated learning. *Knowledge-Based Systems*, 216:106775, 2021.
- Zhao, Y., Li, M., Lai, L., Suda, N., Civin, D., and Chandra, V. Federated learning with non-iid data. *arXiv preprint arXiv:1806.00582*, 2018.
- Zhu, H., Xu, J., Liu, S., and Jin, Y. Federated learning on non-iid data: A survey. *Neurocomputing*, 465:371–390, 2021.

Appendix

The appendix sections display the full hyperparameter settings, method motivation, and additional results for our main experiments.

A. Training Hyperparameters

Table 4 summarizes all hyperparameters that were used for each data set-model configuration throughout all non-IID splits. We train all models for a total of 500 communication rounds, except for ResNet18 on Tiny-ImageNet, which we train for 100 communication rounds. Moreover, we train each setting using a total of 100 clients, of which we select 10 randomly to participate in training in each communication round, except for SimpleCNN on CIFAR-10 where we select 30 out of 100 clients to participate in each round. We evaluate all clients after every ten communication rounds. For CIFAR-10 we train a SimpleCNN with batch size 50 using SGD with a learning rate of 0.02 and a pre-trained SqueezeNet with learning rate of 0.001 and batch size 32. For Tiny-ImageNet we train a pre-trained ResNet18 with batch size 32 using SGD with a learning rate of 0.01, and a MobileNetV2 with batch size 64 and learning rate 0.01. We use SGD as an optimizer with momentum set to 0.9 for all runs except for SimpleCNN on CIFAR-10 where momentum is set to be 0.5. Moreover, we set weight decay to 10^{-4} for all runs except for SimpleCNN on CIFAR-10 where it is set to 0.5, and for SqueezeNet on CIFAR-10 where it is set to 0. For FedProx we set the proximity hyperparameter to $\mu = 0.01$ for SimpleCNN on CIFAR-10, $\mu = 0.1$ for SqueezeNet on CIFAR-10, $\mu = 0.1$ for MobileNetV2 on Tiny-ImageNet, and lastly $\mu = 10^{-3}$ for ResNet18 on Tiny-ImageNet. For SoticFL⁺ we set the local epochs to the same value as epochs for the global model $\tau = E$. We set the cluster number hyperparameter to $S = 10$ for all Dirichlet-based experiments, and to $S = 2$ and $S = 5$ for the 2-Fold and 5-Fold experiments, respectively. The number of samples that we sample on each client for training to $\Omega_{tr} = 1$ for SoticFL and to $\Omega_{tr} = 10$ for SoticFL⁺ and the number of samples for ensembling at test time to $\Omega_{te} = 1$ for both SoticFL and SoticFL⁺. All training hyperparameters for CIFAR-10 on a SimpleCNN where taken from (Hahn et al., 2022), CIFAR-10 on a pre-trained SqueezeNet from (Nguyen et al., 2022), Tiny-ImageNet on a pre-trained ResNet18 from (Chen et al., 2022b), and Tiny-ImageNet on MobileNetV2 from (Shi et al., 2023).

Table 4. Summary of used hyperparameters for training.

Data set/Model	T	K	$ S^t $	e	E/τ	γ	mom.	wd	μ
CIFAR-10/SimpleCNN	500	100	30	50	5	0.02	0.5	0.5	0.01
CIFAR-10/SqueezeNet	500	100	10	32	1	0.001	0.9	0	0.1
TinyImageNet/MobileNetV2	500	100	10	64	5	0.01	0.9	10^{-4}	0.1
TinyImageNet/ResNet18	200	100	10	32	5	0.01	0.9	10^{-4}	10^{-3}

B. Comparison of SoticFL and SoticFL-All

In this preliminary results we show that solution simplex learning is effective if applied only on the classification layer of the model, as opposed to all layers in network. For this, we train a SimpleCNN where all of its layers are parameterized by a solution simplex (SoticFL-All) and compare it to a standard network where only the classification layer is a trained solution simplex (SoticFL). As Figure 9 shows, SoticFL-All yields similar performance than SoticFL wrt. average local test accuracy, however, converges slower. On the other hand, for global test performance, SoticFL-All fails to match the performance of SoticFL and all the baselines.

C. Time-to-accuracy evaluation

Similar to Table 2 and Table 3, we plot the TTA improvement for SoticFL. In particular, we show the TTA improvement of SoticFL over FedAvg, and TTA improvement of SoticFL⁺ over Ditto. All reported results are average values that we computed over 5 different random seeds.

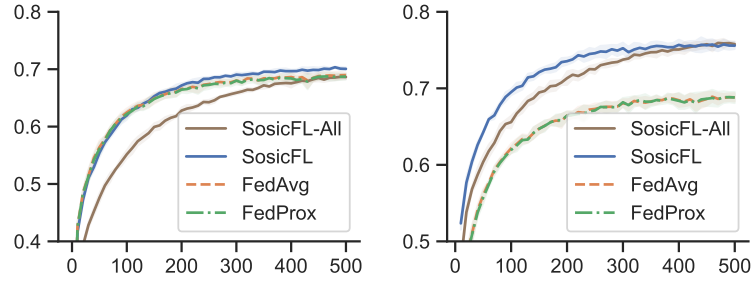


Figure 9. Global (left) and average local (right) test accuracy on CIFAR-10 on the 2-Fold setting and random SimpleCNN initialization. The shown results are averaged over 5 seed runs.

Table 5. Improvements for *global* and *local* TTA for all datasets/models.

	CIFAR-10 on SimpleCNN						TinyImagenet on MobileNet V2					
	2-Fold		5-Fold		Dir(0.5)		2-Fold		5-Fold		Dir(0.3)	
SosicFL	x1.7	x5.0	x1.2	x3.8	x1.2	x1.9	x1.4	x9.8	x1.1	x7.0	x1.8	x2.4
SosicFL ⁺			x1.3	x1.3	x1.6	x1.7			x1.2	x8.6	x2.9	x7.0
	CIFAR-10 on SqueezeNet						TinyImagenet on ResNet18					
	2-Fold		5-Fold		Dir(0.1)		2-Fold		5-Fold		Dir(0.3)	
SosicFL	x1.4	x3.3	x1.4	x3.0	x1.6	x2.9	x1.5	x3.1	x1.2	x2.9	x1.4	x3.2
SosicFL ⁺			x1.2	x1.4	x1.4	x1.4			x1.2	x1.9	x2.0	x1.7